A brief primer on networks in neuroscience

Mark A. Kramer
Boston University
111 Cummington St
Department of Mathematics and Statistics
Boston, MA, 02215

Abstract

Networks now play a prominent role in neuroscience research, supported by new recording and analysis techniques. In this chapter we provide a brief introduction to this emerging field, with particular emphasis on methods to create (structural or functional) networks from neuronal data and measures to characterize structural network properties. We also outline three simple models of networks, including the small-world network. The concepts introduced in this chapter provide a basic foundation to begin further exploration of networks in neuroscience.

Introduction

The appearance of networks in neuroscience has grown tremendously in the past decade, supported by new recording and analysis techniques. To summarize this expanding field is a daunting task and not the goal of this chapter. Instead, we will consider a brief introduction to network analysis, with emphasis on the application of networks to problems in neuroscience. We will focus in particular on techniques to create networks (either functional or structural) from data, tools to analyze networks, and methods to construct simple network models. Again, our goal in this chapter is simply to introduce these concepts and provide the reader with a basic background applicable in later chapters and for further exploration of this emerging field. More detailed discussions of networks and their application may be found in the references (1-5).

Structural and functional networks

Many examples of networks exist in the world. These include structural networks (e.g., the network of roads that connect cities and towns), social networks (e.g., the networks of film actors that collaborate in movies), and biological networks (e.g., a network of neurons connected with synapses or gap junctions). In each case, we can divide the network into two fundamental components: *nodes* (the cities, actors, or neurons) and *edges* (the roads, films, or synapses) that connect node pairs. In what follows, we will focus on *binary, undirected* networks. In these simplified networks, an edge either exists between two nodes or does not, and the presence of an edge provides no directional (i.e., no causal) information.

In neuroscience, networks are typically divided into two categories: structural networks and functional networks (4). In *structural* networks, the edges represent physical

connections between nodes. At the microscopic spatial scale, these include synaptic or gap junctional connections between individual neurons. In neuroscience, the only complete structural network mapped at this scale is for the nematode worm *C. elegans* (6,7). At the macroscopic spatial scale, white matter tracks are used to infer synaptic connections between brain regions and construct structural networks in humans (8-10).

Functional networks rely on the coupling between dynamic activity recorded from separate brain areas. For example, we illustrate in Figure 1A simulated electroencephalogram (EEG) data recorded from two electrodes placed on the scalp surface of a human subject. To construct a simple network from these data (consisting of only two nodes), we determine how well the EEG data recorded at the two electrodes match. Many measures exists to characterize this "match" (or coupling) between EEG signals (11). Here we employ a very simple measure: the cross correlation. The idea of this measure is to compare the two time series and see how well the voltage traces align. In doing so, we compare the signals both directly and shifted in time with respect to one another. Examining how the signals align over different time shifts allows us to detect if one signal is simply a delayed version of another (Figure 1A). When the alignment between the two signals is good the cross correlation approaches 1, while when the alignment is poor the cross correlation approaches 0. If two signals are completely out of phase (e.g., when one reaches its maximum, the other reaches its minimum, and vice versa) the cross correlation approaches -1. Depending on the time shift between the two signals, we may observe all three types of correlation, as we now describe.

The cross correlation between the two simulated EEG recordings varies between -1 and 1 (Figure 1B). With no shift in the signals, the cross correlation is small (near 0). If we delay one signal backwards in time by 25 ms, the two EEG recordings "anti-correlate" (i.e., when one signal peaks, the other troughs) and the cross correlation approaches -1. When we advance one signal (gray in Figure 1A) forward in time by 25 ms, the two EEG recordings align and the cross correlation reaches 0.9. This last result indicates that the voltage activity observed at the two electrodes is coupled: the EEG data exhibit a strong correlation at a specific time shift. We represent this graphically by connecting the two electrodes with an edge (Figure 1C). In doing so, we have created a simple, 2-node network with one edge. The two nodes represent the two EEG electrodes, and the edge indicates sufficiently strong coupling between the voltage activity recorded from the two electrodes.

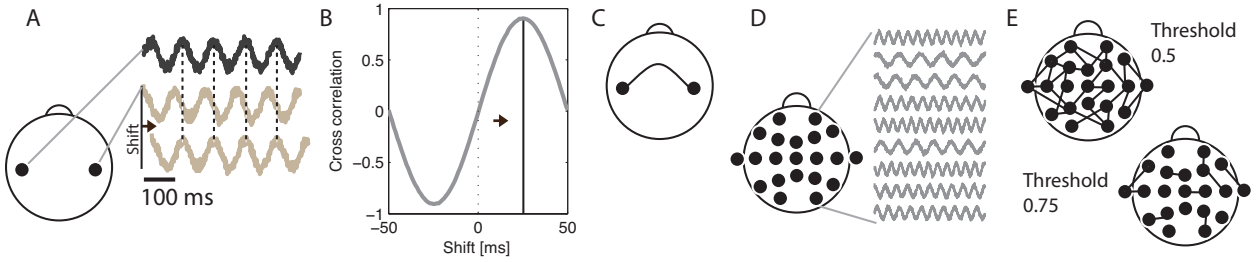

Figure 1: Example method to construct functional networks from voltage data. (A) In this simulated example, EEG data are recorded from two electrodes on the scalp surface; the EEG data (black and upper gray curve) are simple sinusoids with added noise. If we shift the lower (gray) trace to the right by

some time advance, then the EEG data at the two electrodes align. (B) The cross correlation between the two electrodes is large when we shift the EEG data from one electrode by 25 ms. (C) Because the cross correlation is strong enough, we connect the two electrodes with an edge (black line) and form a simple two-node network. (D) Simulated multivariate data recorded from many EEG electrodes, results in (E) a much more complicated network in which the number of edges depends upon the choice of coupling threshold.

This procedure extends to any number of electrodes (for example the 21 electrodes typically used in the 10-20 electrode configuration). In this case, we compute the coupling between the voltage data recorded for all electrode pairs (Figure 1D). We then connect electrode pairs whose coupling exceeds a threshold value (e.g., 0.5) with an edge. As we show in Figure 1E, the connectivity becomes much more difficult to visualize as the number of nodes increases. In fact, as the number of nodes increases, the maximum number of possible edges increases dramatically: the 21-node network could support over 200 edges compared to 1 possible edge in the 2-node network. Simple visual inspection of the network structure, which sufficed for the 2-node network (Figure 1C), becomes inadequate for this larger, more complicated network.

Two subtleties exist in constructing functional networks from time series data. First, what coupling measure is most appropriate? Different measures exist that focus on linear interactions (12-14), nonlinear interactions (15), wavelet coherence (16), causality (17), and many other methods (11). Each measure provides a different view of the coupling and requires different processing methods and assumptions (e.g., filtering the data in a specific frequency band to extract phase information, or choice of embedding dimension). Recent studies suggest that linear and nonlinear coupling measures perform equally well when applied to macroscopic voltage data, although subtle changes in the physiological state of the brain may require more sophisticated coupling measures (18-23).

Second, how do we determine the appropriate coupling threshold? In Figure 1 we connected electrode pairs with edges whose coupling measure (in this case the cross correlation) exceeded a threshold value (e.g, 0.5). No technique yet exists to choose the most appropriate coupling threshold. One approach is to examine the networks produced for a variety of threshold values and seek consistent results (15, 24-30). However, we may find that different threshold values produce extremely different networks (compare the two networks in Figure 1E).

Another approach to defining a coupling threshold is first to apply an appropriate statistical hypothesis test to the coupling result computed for each electrode pair. Doing so, we may then assign a p-value to each edge and threshold these p-values rather than the original coupling measure (31). An advantage of this approach is that multiple comparisons (a p-value exists for each electrode pair) may be addressed using sophisticated statistical techniques (32), and a measure of network uncertainty deduced, namely the number of spurious edges in the network (31). One difficulty of this approach is the development of an appropriate method to determine the statistical significance of the coupling measure. For classical linear measures (such as the coherence or cross correlation), analytic techniques exist to determine the statistical significance of

the measure, although these typically require specific assumptions about the data (e.g., the asymptotic case of extremely large sample sizes). For modern nonlinear measures, no such analytic methods to assess statistical significance exist. Instead one might employ a bootstrapping procedure, however bootstrapping techniques are computationally expensive and typically not tractable for large networks.

Simple measures to characterize network structure

Typically, after constructing a functional network, we analyze its structure. A useful, first analysis is visual inspection of the network (e.g., visual inspection of the networks in Figure 1E). But, as the number of nodes in a network increases, so does the number of possible edges, and visual inspection becomes less useful. For a network of *N* nodes, the maximum possible number of edges is $N(N\text{-}1)/2$. When *N* is large (e.g., in a high density EEG recording with 128 electrodes or a multielectrode array with 100 contacts) the networks typically become much too complicated for visual inspection (Figure 2A,B). To go beyond visual inspection and characterize the structure of these large networks, many measures exist (1,3,5). In this section, we briefly outline three of these measures: the degree, path length, and clustering coefficient.

The *degree* (*d*) is simply the number of edges that touch a node. In Figure 3, we show a five node network, and list the degree of each node (in this case a value of either 2 or 4). To summarize the degree values of the entire network, we compute the average degree ($\underline{D}$) of all nodes, and find in this case 2.4. For much larger networks, the degree distribution is a useful measure that illustrates the probability of observing a node of degree *d* (Figure 2C). In many real-world networks (including the film actor network and neural networks (33)), the degree distribution exhibits a power law: the probability of observing a node of degree *d* decreases as $1/d^{\alpha}$ where α is a positive number (Figure 2D) (2). In these networks high degree nodes (which appear less frequently than the low degree nodes) may serve important functional roles in the network (i.e., may act as hubs) although this is not always the case (34). Degree distributions with power law behavior are also known as scale-free because the degree distribution looks the same (just scaled by a constant value) if we multiply the value of *d* by a constant.

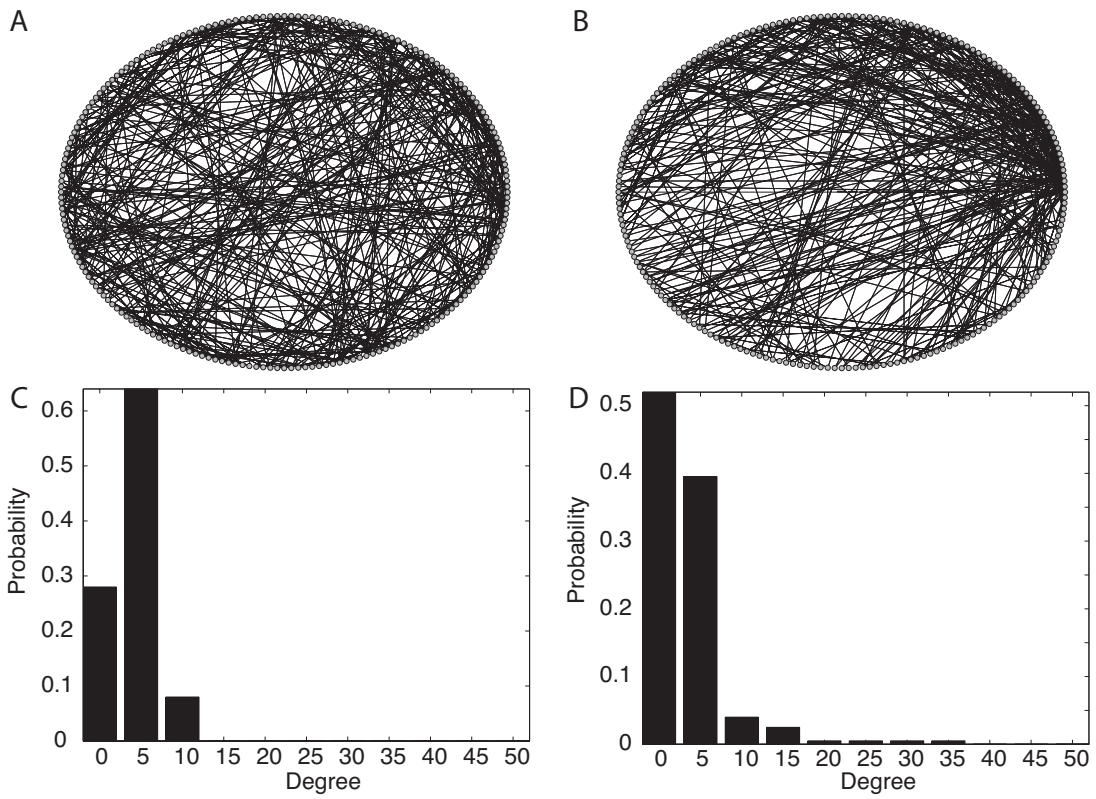

Figure 2: Two larger networks consisting of 200 nodes. (A, B) We arrange the nodes (gray) in the network as a ring, although this does not imply a literal spatial sensor location in the "real" experiment. Each node represents an individual electrode or sensor, and each edge (black line) indicates sufficiently strong coupling between activity recorded simultaneously at two nodes. For such large networks, the network structure becomes much more difficult to characterize through visual inspection. (C, D) The degree distributions for each network. For the network in (A) most of the nodes have a degree near 5. For the network in (B), most of the nodes have a degree less than five, but some nodes have a high degree (up to 35 edges).

The *path length* (*l*) is the minimum number of edges traversed to go from one node to another in the network. We assume here that each node is reachable from any other node; when this is not the case, care must be taken to account for unreachable nodes. In the example 5-node network, the path length from node *i* to any other node is 1; node *i* can reach any other node by traversing 1 edge. Nodes *ii-v* can reach any other node in 1 or 2 steps. We note that many different paths exist between nodes. For example, we can travel directly from node *ii* to node *iii*, or we can pass through node *i* on the way to node *iii*. When computing the path length, by convention we always choose the shortest path between nodes. The *average path length* (*L*) is calculated from the path length between each node and all other nodes in the network; for the 5-node network, the average path length is 1.4.

The final measure we consider is the *clustering coefficient* (*c*). The clustering coefficient of a node is the number of connections that exist between the nearest neighbors

of a node, expressed as a proportion of the maximum number of possible connections between the nearest neighbors of the node. This definition is perhaps best illustrated through an example. In the 5-node network, chose node *ii* and notice that this node has two neighbors (i.e., two nodes directly connected to node *ii* by a single edge, nodes *i* and *iii* in Figure 3B). We now examine whether an edge exists between the two neighbor nodes. In this example, it does (see Figure 3A) so we complete a triangle or cluster in the network. In social networks, clustering is typically high; the friends (nearest neighbors) of an individual (the chosen node) also tend to be friends (i.e., edges connect the nearest neighbors of the chosen node). The formula to compute the clustering coefficient for a node *n* is,

$$c_n = \frac{E(\Gamma_n)}{k_n(k_n-1)/2}$$

Here, Γ_n is a list of the nearest neighbors of node *n*, $E(\Gamma_n)$ is the number of edges between the nearest neighbors of *n* (but does not include edges that connect to node *n* directly), and k_n is the number of nodes in Γ_n. For *n*=*i* in the example 5-node network, Γ_n = {ii,iii,iv,v} and k_n=4. Two edges exist within this neighborhood (between nodes *ii* and *iii*, and between nodes *iv* and *v*), so $E(\Gamma_n)$ = 2. Plugging into the equation above, we find c_i=2/6=1/3. This result indicates that of all the possible completed triangles between the nearest neighbors of node *i*, only one-third exist. To complete all of the triangles between the nearest neighbors of node *i* would require additional connections between nodes *ii* and *iv*, nodes *ii* and *v*, nodes *iii* and *iv*, and nodes *iii* and *v*. For the other nodes, the clustering coefficient equals 1. All possible triangles between the nearest neighbors of these other nodes do exist. The *average clustering coefficient* (*C*) is the average of *c* between all nodes in the network; for the 5-node network *C* is 13/15.

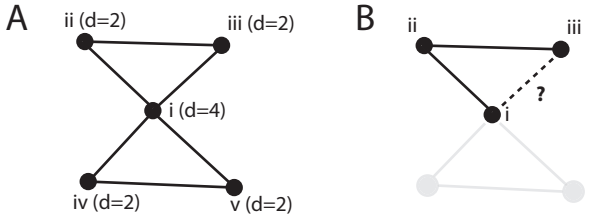

Figure 3: An example 5-node network to illustrate the simple measures of network structure. (A) We label the 5-nodes (circles) with roman numerals and connect the nodes with edges (lines). The number in parentheses next to each node indicates its degree (*d*). (B) To determine the clustering coefficient of node *ii*, we first determine its nearest neighbors (the other two nodes in the network are grayed out). We then determine if an edge exists between these neighbors (the dotted line). Because this edge exists in (A), the three nodes form a triangle or cluster.

In this section we described three measures of network structure. These measures provide simple numeric summaries to characterize complex networks, consisting of many nodes and edges. As an example of the application of these measures, we consider the nervous system of *C. elegans*, which has been completely mapped at the cellular level. The network consists of *N*=282 nodes (or neurons). The average degree *D*=14, average path length *L*=2.65, and average clustering coefficient *C*=0.28 (33). Al-

ready these results reveal some interesting aspects about the network structure (for example, we can travel from one neuron to any other in 3 steps, on average). To further interpret these results, we consider three reference networks described in the next section.

Simple network models

In the previous section, we considered three measures to summarize observed (or constructed) networks. In this section, we consider three simple models to generate networks. For each network, we outline the construction method and provide approximate formulas for the average degree, average path length, and average clustering coefficient.

We start with a *regular network*, in which we arrange the nodes as a ring and connect each node to the k closest nodes on the ring (Figure 4A). The result is a network with mesh-like connections between neighboring nodes. For a regular network of N nodes, approximate formulas exist for the average degree, average path length, and average clustering coefficient. The expression for the average degree is $\underline{D}=k$. In a regular network, the same number of edges connect to each node. The expression for the average path length is $\underline{L}\sim N/(2k)$. As the number of nodes (N) increases, so does the average path length; in a large network (when N is big), we must travel many edges (from neighbor to neighbor around the circumference of the circle in Figure 4A) to reach our destination. Finally, the average clustering coefficient is a constant: $\underline{C}\sim 3/4$ for large k. In the regular network, the mesh-like connections between nodes establish many clusters (or triangles).

The second model network we consider is a traditional *random network*. In this network, we connect each pair of nodes with probability p. To construct this network, we imagine flipping a (perhaps biased) coin for each node pair. If the coin flip results in heads, we connect the two nodes with an edge, otherwise we do not (Figure 4C). Approximate formulas for the network measures exist for a random network of N nodes as well. The average degree is $\underline{D}\sim p(N-1)$, the probability of success (p) multiplied by the number of times we flip the biased coin for each node (note that, in a network of N nodes with no self connections, each node can connect to N-1 other nodes). The average path length, $\underline{L}\sim \ln(N)/\ln(\underline{D})$, increases as the number of nodes increases, although not as quickly as in the regular network. Finally, the average clustering coefficient, $\underline{C}\sim \underline{D}/N$, decreases as the number of nodes N increases; clusters (or triangles) appear infrequently in random networks.

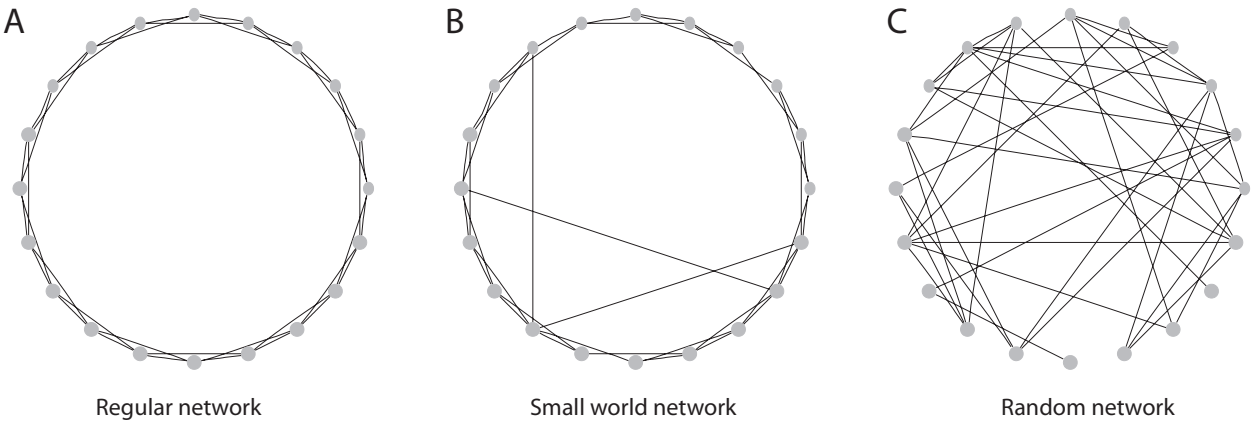

Figure 4: Examples of a regular network, small world network, and random network (N=20 and $\underline{D}$=4). In the regular network (A), mesh-like connections occur between neighboring nodes. In the small world network (B), most connections are local, but a few long distance connections exist. These few shortcuts dramatically decrease the average path length of the network, without impacting the clustering coefficient substantially. In the random network (C), edges occur between node pairs with equal probability.

To illustrate the differences between a regular and random network, consider N=20 nodes and $\underline{D}$=4. Using the formulas above, we find a larger average path length for the regular network ($\underline{L}$~2.5) compared to the random network ($\underline{L}$~2.16). To travel from one node to another in the regular network, we might imagine proceeding from neighboring node to neighboring node around the circumference of a circle (Figure 4A). Travel in the random network typically requires fewer steps because connections span the middle of the circle; no longer is travel restricted to the circle circumference (Figure 4C).

For this same example (N=20 nodes and $\underline{D}$=4), we find a much larger clustering coefficient for the regular network ($\underline{C}$~0.75) compared to the random network ($\underline{C}$~0.2). In the random network, the nearest neighbors of a node are no more likely to be connected than any other nodes; the probability that a node's "friends" are also friends in a random network is p. In the regular network, the mesh-like structure of the connections supports completed triangles (i.e., clusters).

Is either the regular or random network a good approximation to the *C. elegans* neural network? To address this, we fix N=282 and $\underline{D}$=14 (the values for *C. elegans* (33)), compute the average path length and average clustering coefficients for the corresponding regular and random networks, and compare these values to those determined for the observed neural network in Table I.

Table 1: The average path length ($\underline{L}$) and average clustering coefficient ($\underline{D}$) for the *C. elegans* neural network and for a regular and random network with the same number of nodes and average degree (33).

	C. elegans	Regular	Random
$\underline{L}$	2.65	10	2.13

$\underline{C}$	0.28	0.75	0.05

These calculations suggest that the average path length of the *C. elegans* network is better approximated by a random network; the average path length of both networks is considerably shorter than that for a regular network. Yet, we find that the clustering coefficient of the *C. elegans* network is poorly approximated by the random network. The *C. elegans* network possesses a higher clustering coefficient, which is better approximated by the regular network. We conclude that neither the regular nor random network accurately represents both the clustering coefficient and average path length calculated for the *C. elegans* network. Each models captures only one important aspect of the network topology.

The final model we consider — the small world network — provides a better approximation to the *C. elegans* network. Like this neural network, the small world network possesses both a small average path length and a large average clustering coefficient. We construct the small world network in the following way (33). First, we begin with a regular network of N nodes each with k edges. We then rewire each edge with probability p. More specifically, we choose an edge, flip a biased coin (with a probability of success p), and if the flip is successful, we disconnect one end of the edge and reconnect it to another node chosen at random (with uniform probability) from all other nodes. When p is small, the result is a rewiring of a few network edges (Figure 4B). These edges typically serve as network shortcuts; we can follow these edges to quickly move from one side of the network to the other. The result of these few shortcuts is a dramatic decrease in the average path length. However, because we rewire only a few edges, the average clustering coefficient of the network remains large. These are the characteristics of a small world network: a few shortcuts create a network with small average path length and large average clustering coefficient.

Brain networks (both structural and functional) appear frequently to possess small world structure (35-38). We might interpret these observation as the brain seeking to balance segregation of information processing to local structures and integration of this processing between distant structures (4). In attempting to achieve this balance, perhaps the brain seeks to minimize wiring (therefore making most connections local) and maximize efficiency (so that signals may travel quickly from one brain region to another through a minority of large distance connections). These reasonable arguments make the small world network a compelling model of brain networks.

Conclusions

The application of networks to problems in neuroscience is rapidly expanding. The emergence of new technology (e.g., high-density multielectrode array recordings from thin slices of brain tissue *in vitro* or diffusion tensor imaging of white matter tracks *in vivo*) permits unprecedented collection of neuronal network data. Characterizing these networks — and understanding their implications for brain function — will require the continued development of mathematical tools and theory.

In this chapter, we considered two types of networks studied in neuroscience: structural networks and functional networks. Both types of networks undoubtably serve important roles in the brain. Structural networks form the backbone of neural connectivity, while functional networks make dynamic use of this backbone and transiently unite disparate brain regions. Although we distinguished between these two types of networks, dynamic brain activity (resulting in functional connections) alters brain structural connectivity (through plasticity mechanisms, for example); in other words, brain structural and functional connectivity are interrelated.

We conclude with suggested questions to consider when examining networks in neuroscience literature (Table 2). Each question focuses on topics considered in this primer, which provides only a brief introduction to the field of networks. Many other network measures exist beyond the three discussed here (e.g., betweenness or assortativity). Similarly, other network models exist (e.g., preferential attachment) beyond the regular, random, and small world networks. Nevertheless, we hope this brief introduction has prepared (and motivated) readers to pursue further study in this growing field.

Table 2: Suggested questions to consider when exploring networks in the neuroscience literature

1. Is the network *structural* or *functional*?
2. If the network is functional:
a. What coupling method determined node connectivity?
b. What coupling *threshold* defined the edges?
3. What is the average degree, average path length, and average clustering coefficient?
4. Is the network approximately *regular*, *random*, or *small world*?

References

1. Wasserman S, Faust K. Social Network Analysis: Methods and Applications. Cambridge University Press; 1994.
2. Albert R, Barabási A. Statistical mechanics of complex networks. Reviews of Modern Physics. 2002 Jan;74:47–97.
3. Newman M. The Structure and Function of Complex Networks. SIAM Review. 2003;45(2):167.
4. Bullmore E, Sporns O. Complex brain networks: graph theoretical analysis of structural and functional systems. Nat Rev Neurosci. 2009 Mar;10(3):186–98.
5. Kolaczyk ED. Statistical Analysis of Network Data: Methods and Models. Springer; 2009.
6. White J, Southgate E, Thomson J, Brenner S. The Structure of the Nervous System of the Nematode Caenorhabditis elegans. Philos T Roy Soc B. 1986 Nov;314(1165):1–340.

7. Achacoso TB, Yamamoto WS. AYs Neuroanatomy of C Elegans for Computation. CRC-Press; 1992.
8. Iturria-Medina Y, Canales-Rodríguez EJ, Melie-García L, Valdés-Hernández PA, Martínez-Montes E, Alemán-Gómez Y, et al. Characterizing brain anatomical connections using diffusion weighted MRI and graph theory. Neuroimage. 2007 Jul;36(3):645–60.
9. Iturria-Medina Y, Sotero RC, Canales-Rodríguez EJ, Alemán-Gómez Y, Melie-García L. Studying the human brain anatomical network via diffusion-weighted MRI and Graph Theory. Neuroimage. 2008 Apr;40(3):1064–76.
10. Hagmann P, Cammoun L, Gigandet X, Meuli R, Honey C, Wedeen V, et al. Mapping the Structural Core of Human Cerebral Cortex. PLoS Biology. 2008 Jul;6(7):e159 EP.
11. Pereda E, Quiroga R, Bhattacharya J. Nonlinear multivariate analysis of neurophysiological signals. Prog Neurobiol. 2005 Jan;77:1–37.
12. Brazier MA. Electrical seizure discharge within the humn brain: the problem of spread. In: Braizer MA, editor. Epilepsy, its phenomenon in man. Academic Press; 1973. .
13. Tharp BR, Gersch W. Spectral analysis of seizures in humans. Comput Biomed Res. 1975 Dec;8(6):503–21.
14. Mitra P, Bokil H. Observed Brain Dynamics. Oxford University Press; 2008.
15. Ponten SC, Bartolomei F, Stam CJ. Small-world networks and epilepsy: graph theoretical analysis of intracerebrally recorded mesial temporal lobe seizures. Clin Neurophysiol. 2007 Apr;118(4):918–27.
16. Lachaux JP, Lutz A, Rudrauf D, Cosmelli D, Quyen MLV, Martinerie J, et al. Estimating the time-course of coherence between single-trial brain signals: an introduction to wavelet coherence. Clin Neurophysiol. 2002;32(3):157–174.
17. Kamiski M, Ding M, Truccolo WA, Bressler SL. Evaluating causal relations in neural systems: granger causality, directed transfer function and statistical assessment of significance. Biol Cybern. 2001 Aug;85(2):145–57.
18. Aarabi A, Wallois F, Grebe R. Does spatiotemporal synchronization of EEG change prior to absence seizures? Brain Res. 2008 Jan;1188:207–221.
19. Ansari-Asl K, Senhadji L, Bellanger JJ, Wendling F. Quantitative evaluation of linear and nonlinear methods characterizing interdependencies between brain signals. Phys Rev E. 2006 Sep;74(3 Pt 1):031916.
20. Kreuz T, Mormann F, Andrzejak R, Kraskov A, Lehnertz K, Grassberger P. Measuring synchronization in coupled model systems: A comparison of different approaches. Physica D. 2007;225(1):29–42.
21. Mormann F, Kreuz T, Rieke C, Andrzejak R, Kraskov A, David P, et al. On the predictability of epileptic seizures. Clin Neurophysiol. 2005;116(3):569–587.

22. Osterhage H, Mormann F, Staniek M, Lehnertz K. Measuring synchronization in the epileptic brain: A comparison of different approaches. Int J Bifurcat Chaos. 2007;17(10):3539–3544.
23. Quiroga RQ, Kraskov A, Kreuz T, Grassberger P. Performance of different synchronization measures in real data: a case study on electroencephalographic signals. Phys Rev E. 2002 Apr;65(4 Pt 1):041903.
24. Stam CJ. Functional connectivity patterns of human magnetoencephalographic recordings: a 'small-world' network? Neurosci Lett. 2004 Jan;355(1-2):25–8.
25. Micheloyannis S, Pachou E, Stam CJ, Vourkas M, Erimaki S, Tsirka V. Using graph theoretical analysis of multi channel EEG to evaluate the neural efficiency hypothesis. Neurosci Lett. 2006 Jul;402(3):273–7.
26. Srinivas K, Jain R, Saurav S, Sikdar S. Small-world network topology of hippocampal neuronal network is lost, in an in vitro glutamate injury model of epilepsy. Eur J Neurosci. 2007 Jan;25(11):3276–86.
27. Stam CJ, Jones BF, Nolte G, Breakspear M, Scheltens P. Small-world networks and functional connectivity in Alzheimer's disease. Cereb Cortex. 2007 Jan;17(1):92–9.
28. Kramer MA, Kolaczyk ED, Kirsch HE. Emergent network topology at seizure onset in humans. Epilepsy Res. 2008 May;79(2-3):173–86.
29. Supekar K, Menon V, Rubin D, Musen M, Greicius M. Network Analysis of Intrinsic Functional Brain Connectivity in Alzheimer's Disease. PLoS Comp Bio. 2008;4(6):e1000100 EP.
30. Yamasaki K, Gozolchiani A, Havlin S. Climate networks around the globe are significantly affected by El Niño. Phys Rev Lett. 2008 Jun;100(22):228501.
31. Kramer MA, Eden UT, Cash SS, Kolaczyk ED. Network inference with confidence from multivariate time series. Phys Rev E. 2009 Jun;79(6 Pt 1):061916.
32. Storey JD, Tibshirani R. Statistical significance for genomewide studies. Proc Natl Acad Sci. 2003 Aug;100(16):9440–9445.
33. Watts DJ, Strogatz SH. Collective dynamics of small-world networks. Nature. 1998 Jun;393(6684):440–2.
34. Doyle J, Alderson D, Li L, Low S, Roughan M, Shalunov S, et al. The "robust yet fragile" nature of the Internet. Proc Natl Acad Sci USA. 2005 Oct;102(41):14497–14502.
35. Song S, Sjöström PJ, Reigl M, Nelson S, Chklovskii DB. Highly nonrandom features of synaptic connectivity in local cortical circuits. PLoS Biol. 2005 Mar;3(3):e68.
36. Kaiser M, Hilgetag CC. Nonoptimal component placement, but short processing paths, due to long-distance projections in neural systems. PLoS Comput Biol. 2006 Jul;2(7):e95.

37. Achard S, Salvador R, Whitcher B, Suckling J, Bullmore E. A resilient, low-frequency, small-world human brain functional network with highly connected association cortical hubs. J Neurosci. 2006 Jan;26(1):63–72.
38. Bassett DS, Bullmore E. Small-world brain networks. The Neuroscientist : a review journal bringing neurobiology, neurology and psychiatry. 2006 Dec;12(6):512–23.